



## Characterization of membrane electrode assemblies in polymer electrolyte fuel cells using a.c. impedance spectroscopy<sup>☆</sup>

N. WAGNER

Deutsches Zentrum für Luft- und Raumfahrt e.V. (DLR) Institut für Technische Thermodynamik, Pfaffenwaldring 38-40, D-70569 Stuttgart, Germany; e-mail: norbert.wagner@dlr.de

Received 22 June 2001; accepted in revised form 5 March 2002

**Key words:** current–voltage curves, electrochemical impedance spectroscopy (EIS), membrane–electrode assemblies (MEA), polymer electrolyte membrane fuel cell (PEFC)

### Abstract

The most common methods used to characterize the electrochemical performance of fuel cells are to record current–voltage  $U(i)$  curves. However, separation of electrochemical and ohmic contributions to the  $U(i)$  characteristics requires additional experimental techniques. The application of electrochemical impedance spectra (EIS) is an approach to determine parameters which have proved to be indispensable for the development of fuel cell electrodes and membrane electrode assemblies (MEAs). This paper proves that it is possible to split the cell impedance into electrode impedances and electrolyte resistance by varying the operating conditions of the fuel cell (current load) and by simulation of the measured EIS with an equivalent circuit. Furthermore, integration in the current density domain of the individual impedance elements enables the calculation of the individual overpotentials in the fuel cell and the determination of the voltage loss fractions.

### 1. Introduction

Fuel cells offer a highly efficient and environmentally friendly technology for energy conversion avoiding the limitations of Carnot cycle. Polymer membrane fuel cells (PEFC) are considered as one of the most promising options for powering future cars [1] and small combined power units due to their modular construction and the high energy densities that can be attained.

An important research and development goal is to increase the efficiency and to produce efficient, cheap electrodes and membrane–electrode assemblies (MEA). There is a need for production technologies of PEFC electrodes and MEAs that allows mass production of reproducible electrodes [2, 3]. In order to improve the efficiency of the fuel cell systematically a better understanding of the electrochemical reactions and mass transport in the fuel cell is essential. Moreover, quality control and understanding of degradation require new nondestructive methods and a better understanding of experimental results based on modelling and simulation.

### 2. Experimental details

The PEFC operates between 50 °C to 80 °C with a proton exchange polymer membrane (e.g., Nafion<sup>®</sup> 117) as electrolyte. The overall electrochemical reactions are: oxidation of hydrogen and reduction of oxygen forming water as reaction product at the cathode.

The PEFC electrodes were commercial electrodes from E-TEK (20% Pt/C, 0.4 mg cm<sup>-2</sup>, thickness 200 μm), impregnated with 1 mg cm<sup>-2</sup> Nafion<sup>®</sup> suspension from Aldrich Chemie, with Nafion<sup>®</sup> 117 as electrolyte membrane. After pretreatment of the Nafion membrane with H<sub>2</sub>O<sub>2</sub>/H<sub>2</sub>SO<sub>4</sub>, electrodes and membrane were hot pressed at 160 °C and 1.6 MPa for 2 min after 8 min heating. Since the resistance of the proton exchange membrane (electrolyte) shows a strong dependence on water content [4] the fuel cell was operated at 80 °C with the hydrogen feed stream humidified by passing through a wash bottle at a temperature of 90 °C. The oxygen was not humidified before entering the cell at room temperature. Both hydrogen and oxygen pressures were kept constant at 2.0 bar absolute. The hydrogen flow was ‘dead end’ whereas the oxygen flow rate was manually adjusted to  $\lambda = 8$  ( $\lambda$  is the factor of the stoichiometric requirement for the applied current) for all current densities to ensure steady state conditions during the impedance measurement. The geometric surface of the electrodes used was 23 cm<sup>2</sup>.

<sup>☆</sup>This paper was initially presented at the 5th International Symposium on Electrochemical Impedance Spectroscopy at Marilleva, Trento, Italy, June 2001.

Electrochemical characterization of the fuel cell was performed by electrochemical impedance measurements in the frequency range 10 mHz to 100 kHz (IM6, Zahner-elektrik, Kronach, Germany). Measurements at currents up to 25 A were carried out in combination with an electronic load (EL101, Zahner-elektrik). It is important to know, that the high range of EIS is limited to frequencies <100 kHz using high current electronic loads. This general limitation in the upper frequency range is caused by limited time constants of the electronic amplifiers, low impedance of the fuel cells (at the used fuel cell typically 5 m $\Omega$ ) and increased inductivity of high current wiring.

Before starting each impedance measurement the cell was prepolarized for at least 15 min at the measuring potential to reach steady state conditions. The current densities before and after measurement were measured to prove stability of the cell during measure times. The d.c. current–voltage values have been used to plot steady state current–voltage curves.

Applying a three electrode cell with one reference electrode is extremely difficult for the investigation of electrochemical systems with solid electrolytes. Therefore, the anode and cathode transfer functions at open circuit potential (OCR) were determined independently without a reference electrode using a symmetrical gas supply of hydrogen and oxygen at the two electrodes of the cell. Thus, cathode and anode impedance at OCP was determined directly with two independent experiments. These results were used to derive appropriate equivalent circuits for the analysis of impedance spectra measured on fuel cells operating with H<sub>2</sub>/O<sub>2</sub>. Furthermore, by varying the experimental conditions such as current load (results presented in this paper), temperature [5], gas composition [6] and humidification [7] measured cell impedance can be split up into anode impedance, cathode impedance and electrolyte resistance without using reference electrodes. The variation of the experimental conditions is also a useful method to confirm the accuracy of the equivalent circuit.

The measured impedance spectra can be described by a model (equivalent circuit) of elementary impedance elements. The numeral values of the parameters are calculated by a fitting procedure of the model to the measured data. The measured data are represented in the following diagrams as symbols and the modelled curves as lines. The equivalent circuit contains various elementary impedance elements representing the reaction and mass transfer steps. These elements are generally represented as ohmic, capacitive or inductive components with particular dependencies of their complex impedance upon the frequency of the a.c. signal. The particular combination of these impedance elements is based on the relationship between the processes represented by these elements. Subsequently occurring steps are represented by a series connection of the elements while steps occurring simultaneously are represented by a connection in parallel. In the case of porous electrodes the connection of the elements is more complicated [8].

### 3. Results

Preliminary impedance spectra (Figure 1) measured at open cell voltage with symmetrical gas supply (H<sub>2</sub>/H<sub>2</sub> and O<sub>2</sub>/O<sub>2</sub>) at 80 °C with impregnated (1 mg cm<sup>-2</sup> Nafion<sup>®</sup> suspension, Aldrich Chemie) E-TEK-electrodes, have shown that the impedance in the low frequency range is much higher when operated symmetrically with oxygen (symmetrical cathode arrangement) than the impedance when the fuel cell is operated symmetrically with hydrogen (symmetrical anode arrangement).

The impedance spectra of the fuel cell operated with symmetrical oxygen supply (curve  $\square$  in Figure 1) and with symmetrical hydrogen supply (curve  $\circ$  in Figure 1) can be simulated by the simplest equivalent circuit (Figure 3(a)) for an electrode–electrolyte interface: charge transfer resistance ( $R_{ct}$ )/double layer capacity in series with the membrane (electrolyte) resistance. The inductance of the wires was not considered in the equivalent circuits.

The charge transfer resistance at open cell voltage is defined by Equation 1:

$$R_{ct} = \frac{RT}{zFi_0} \quad (1)$$

with  $z$  the number of electrons involved in overall reaction,  $i_0$  the exchange current density,  $R$  the gas constant,  $T$  the temperature and  $F$  the faradaic constant.

Fitting the measured impedance data with the equivalent circuit from Figure 3(a) the charge transfer resistances of the cathode and anode can be obtained. Using Equation 1 apparent exchange current densities, without correction for the roughness (porous) surface, temperature, gas pressure, related to the geometric area of the electrodes can be calculated:  $i_{0,\text{anode}} = 0.1 \text{ A cm}^{-2}$  and  $i_{0,\text{cathode}} = 6 \mu\text{A cm}^{-2}$ . Thus, we can conclude that the cell impedance of a fuel cell (H<sub>2</sub>/O<sub>2</sub>) at open circuit potential (OCP) is mainly determined by the charge transfer resistance of the cathode and can be simulated

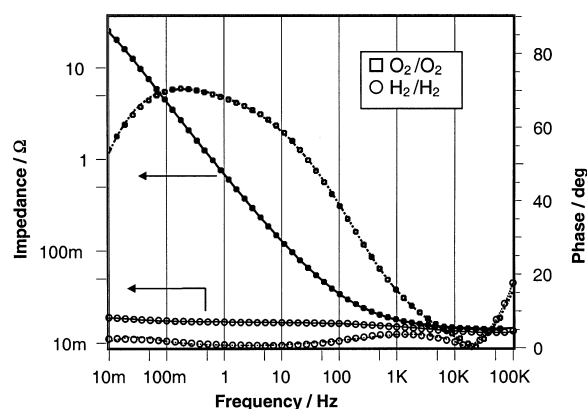


Fig. 1. Bode diagram of the measured impedance spectra, PEFC (hot-pressed, Nafion-impregnated E-TEK electrodes) at 80 °C, at  $p_{\text{H}_2}$  and  $p_{\text{O}_2} = 2$  bar absolute, symmetrical gas supply, OCP.

with the model (Figure 3(b)) obtained after combination of the individual models (Figure 3(a)) for the anode ( $H_2$ ) and cathode ( $O_2$ ), respectively.

EIS measured on the PEFC ( $H_2/O_2$ ) in the potential range from OCP (984 mV) to 697 mV (Figure 2(a)) show an exponential potential dependency due to the high activation energy of the oxygen reduction reaction in the low frequency range. We found only charge transfer reactions, without any diffusion processes in this potential region. The cell impedance at frequencies higher than 10 kHz can be related to the membrane resistance. Current–voltage curves, obtained from the current–voltage values before starting the impedance measurements, indicate a diffusion process at higher current densities. In this case, the measured cell impedances show a minimum at approx. 5.6 A ( $243 \text{ mA cm}^{-2}$ ), 697 mV cell voltage in the low frequency range of the spectra. With further increasing current density, an increase in the cell impedance is observed (Figure 2(b)) and an additional phase-shift maximum at 75 mHz occurs. From this increase in the cell impedance, we can deduce that at higher load of the cell an additional overvoltage occurs. From the correlation of the imped-

ance spectra with the model (Figure 3(c)) we can identify this additional overvoltage as a finite diffusion overvoltage, corresponding to the “Nernst-impedance” frequency behaviour [7, 9–11].

Given the time constant for mass transport, the impedance related to the diffusion is usually found in the lowest frequency region. Therefore, the impedance has to be measured over a wide frequency range, down to 10 mHz, or even lower. To identify and separate the different diffusion processes, it is useful to represent the measured impedance spectra as a Nyquist diagram (imaginary part against real part of the impedance). In the Nyquist diagram one can observe the finite diffusion as an additional loop at the lowest part of the frequency range and the infinite diffusion as a straight line with a slope of 1 (real part = imaginary part). In the Bode diagram (e.g., Figure 2(b)) the difference between the two kinds of diffusion cannot be seen so clearly due to the logarithmically scale. In general, the Bode plot provides a clearer description of the electrochemical system’s frequency-dependent behaviour than the Nyquist plot, in which frequency values are implicit.

To evaluate the measured impedance spectra, the reaction steps can be translated into an appropriate equivalent circuit (EC) which contains various impedance elements representing the reaction steps. An equivalent circuit can be applied for the simulation of the measured impedance spectra of the PEFC. Besides a

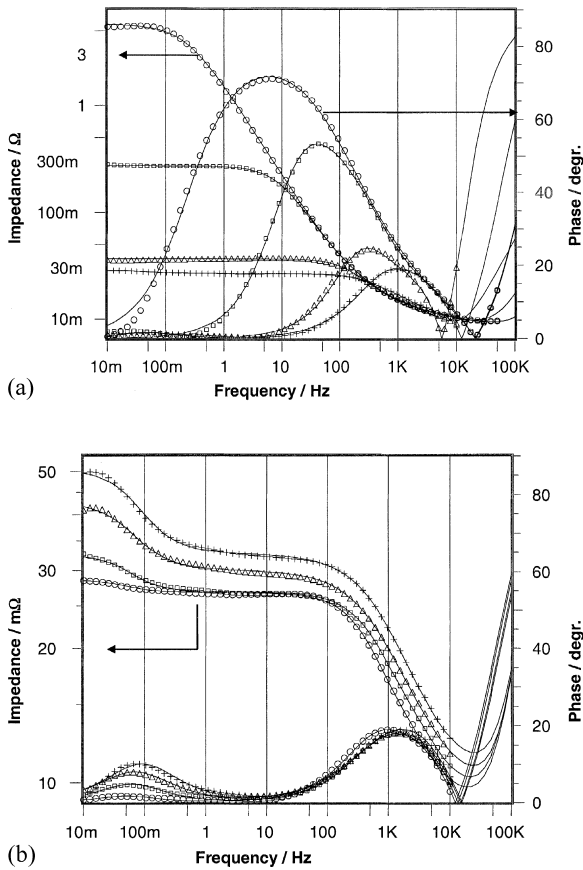


Fig. 2. (a) Bode diagram of the measured impedance spectra, PEFC (hot-pressed, Nafion-impregnated E-TEK electrodes) at 80 °C, at different cell voltages: (○) OCV (984 mV), (□) 900 mV, (△) 797 mV, (+) 697 mV. (b) Bode diagram of the measured impedance spectra, PEFC (hot-pressed, Nafion-impregnated E-TEK electrodes) at 80 °C, at different cell voltages: (○) 697 mV, (□) 597 mV, (△) 497 mV and (+) 397 mV.

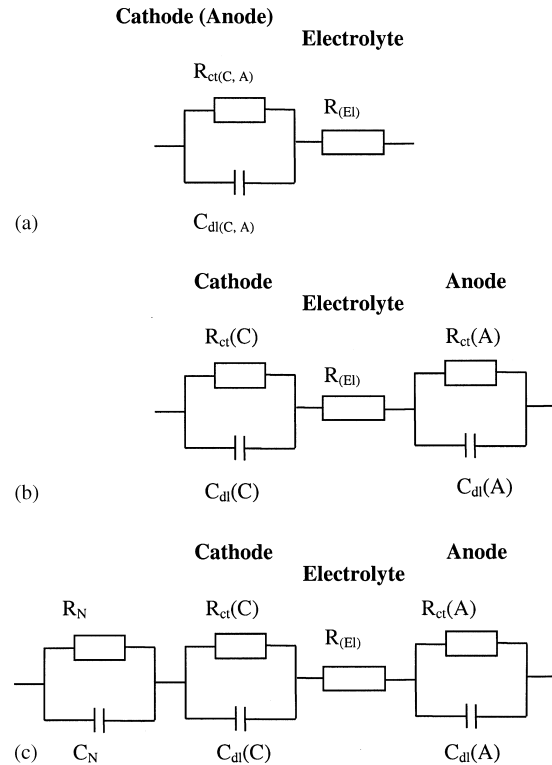


Fig. 3. (a) Equivalent circuits (EC) of the PEFC with symmetrical anode and symmetrical cathode arrangement. (b) Equivalent circuit of the PEFC with  $O_2/H_2$  gas supply, for low current densities. (c) Equivalent circuit of the PEFC with  $O_2/H_2$  gas supply, for high current densities with an additional diffusion step (Nernst-impedance).

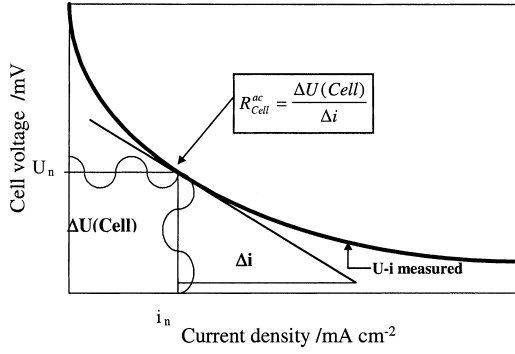


Fig. 4. Schematically representation of the correlation between impedance of fuel cell and  $U/i$  curve.

series resistance (electrolyte resistance  $R_{el}$ ), the equivalent circuit (Figure 3(c)) contains 3 time constants of parallel  $R/C$ . In the simulation the capacitance ( $C$ ) was replaced by  $CPE$  (constant phase element) due to the porous structure of the electrodes. The cathode can be described using two time constants, one for the charge transfer through the double layer ( $R_{ct(C)}/CPE_{dl(C)}$ ), the exponent of the  $CPE$  is around 0.85, for an exponent of 1 the  $CPE$  is equal with the capacitance) and one for the finite diffusion of water with a Nernst impedance-like behaviour ( $R_{(N)}/CPE_{(N)}$ ), the exponent of the  $CPE$  is around 0.95). The time constant of the anode ( $R_{ct(A)}/CPE_{dl(A)}$ ), the exponent of the  $CPE$  is around 0.80) is given by the charge transfer through the anode double layer.

The correlation between impedance measurements and  $U/i$  curves is given schematically in Figure 4. The polarization resistance of the cell measured at  $U_n$  corresponds to the tangent to the  $U/i$  curve at that potential. The polarization resistance of the cell ( $R_{cell}$ ) is the impedance at frequencies near 0 Hz where only ohmic parts attract attention. Obtaining the polarization resistance of the cell, requires extrapolation from the simulated EIS the impedance at very low frequency (e.g., 1 nHz) or summing the individual resistances, obtained after fitting the measured spectra with an equivalent circuit. Assuming that the  $U/i$  curve can be expressed by Equation 2, a second order equation, and the resistance is defined by Equation 3, then the parameters  $a_n$ ,  $b_n$  and  $c_n$  from Equation 2 are given by the Equations 4–6.

$$U_n = a_n I_n^2 + b_n I_n + c_n \quad (2)$$

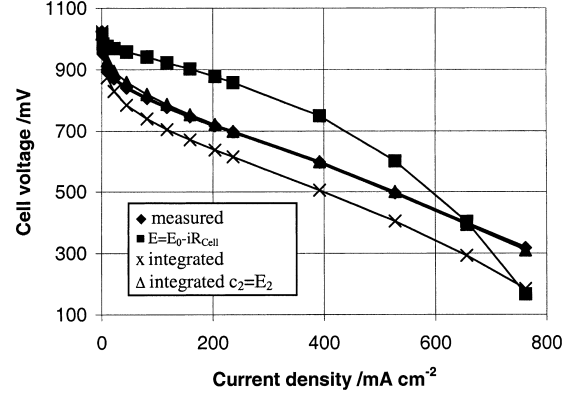


Fig. 5. Measured (◆) and calculated (Equation 2)  $U/i$  curve of the PEFC at 80 °C: (△), with changed boundary condition (×) and  $E = E_0 - iR_{cell}$  (■).

$$R_n = \left. \frac{\partial U}{\partial I} \right|_n \quad (3)$$

with:

$$a_n = \frac{R_{n+1} - R_n}{2(I_{n+1} - I_n)} \quad (4)$$

$$b_n = R_{n+1} - 2a_n I_{n+1} \quad (5)$$

$$c_n = U_{n-1} - a_n I_{n-1}^2 - b_n I_{n-1} \quad (6)$$

Figure 5 shows the measured  $U/i$ -curve. The measured values represent the current density and potential immediately before each EIS measurement after prepolarization. The  $U/i$  curves were calculated using the polarization resistances ( $Z_{1 \text{ nHz}}$ ) after extrapolating the simulated cell impedance to 1 nHz, integrated with Equation 2.

In Table 1 the measured and calculated cell voltages at different current densities and the parameters  $a_n$ ,  $b_n$  and  $c_n$  according to Equations 4–6 are given.

The deviation of the calculated curve from the measured curve can be minimized by fixing  $c_2 = E_2$  (to minimize the error of the integration algorithm, curve (×) in Figure 5) or by increasing the number of measurements, particular in the low current density range where the  $U/i$  curve shows a high deviation from linearity. A large difference between the simulation and the measured  $U/i$  curve is observed assuming a linear

Table 1. Measured and calculated (according to Equation 2) cell voltages at different current densities

| $n$ | $E_{\text{meas.}}/V$ | $i/\text{mA cm}^{-2}$ | $a$       | $b$         | $c$    | $E_{\text{calc.}}/V$ | $Z_{1 \text{ nHz}}/\Omega$ |
|-----|----------------------|-----------------------|-----------|-------------|--------|----------------------|----------------------------|
| 1   | 0.984                | 0.004                 | -21.80816 | 5.85192718  | -0.984 | -0.97826166          | 5.80900                    |
| 2   | 0.900                | 5.814                 | -0.06167  | 0.28917462  | -0.900 | -0.86402335          | 0.27340                    |
| 3   | 0.797                | 93.00                 | -0.00117  | 0.04161802  | -0.869 | -0.78907483          | 0.03683                    |
| 4   | 0.697                | 254.4                 | 0.00060   | 0.02179617  | -0.836 | -0.69537445          | 0.02852                    |
| 5   | 0.597                | 405.0                 | 0.00209   | -0.00466122 | -0.735 | -0.61059086          | 0.03250                    |
| 6   | 0.497                | 516.8                 | 0.00172   | 0.00358358  | -0.779 | -0.51582694          | 0.04276                    |
| 7   | 0.397                | 622.1                 | 0.00185   | 0           | -0.755 | -0.40825618          | 0.05074                    |

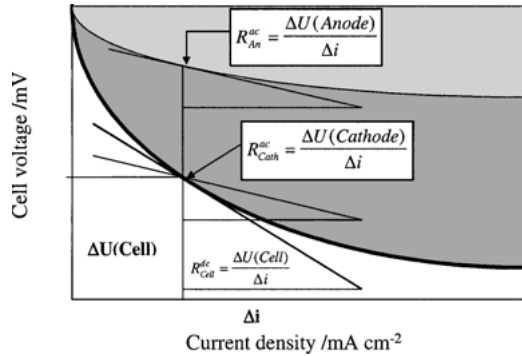


Fig. 6. Schematically representation of the correlation between polarization resistances (anode, cathode and cell) and  $U/i$  curves.

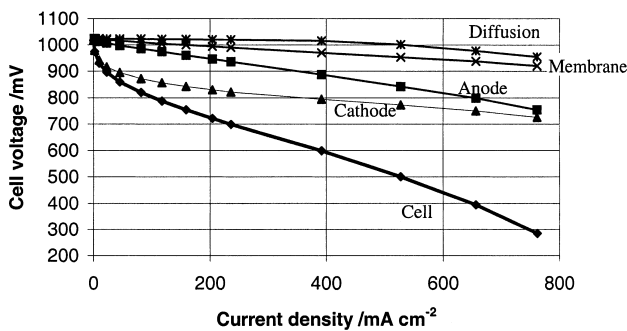


Fig. 7. Cell voltage and individual  $U/i$  curves of the PEFC (hot-pressed, Nafion-impregnated E-TEK electrodes) at 80 °C in function of current density, calculated by integration of the individual resistances at different current densities.

dependency of the cell voltage with current density (curve ■ with  $E_{\text{cell}} = E_0 - iR_{\text{cell}}$ ).

Using the electrode resistances ( $R_{\text{anode}}$  and  $R_{\text{cath}}$ ) gained from the simulation with an equivalent circuit the individual  $U/i$  curves can be determined, as schematically shown in Figure 6.

Figure 7 shows the individual  $U/i$  curves and the cell  $U/i$  curve as a function of current density, calculated by integration of the individual resistances from the equivalent circuit (Figure 3(c)) and the cell resistance at different current densities. At low current densities the cell overpotential is given mainly by the cathodic overpotential. At higher current densities ( $i > 400 \text{ mA cm}^{-2}$ ) an additional diffusion overpotential becomes notice-

able. The increase in the anodic overpotential with increasing current density can be explained by assuming a partially dry out of the interface membrane/anode and can be minimized by appropriate water management.

By increasing the number of impedance measurements, a very good agreement between the measured and calculated  $U/i$  curves can be obtained.

#### 4. Conclusion

Electrochemical impedance spectroscopy is very useful method for the characterization of fuel cells. By varying the operating conditions, such as cell potential or current density and gas supply, the cell impedance can be split into electrode impedances and electrolyte resistance. Furthermore, the electrode impedances can be separated into different impedances representing different reaction steps. Integration over the current densities of the individual impedance elements enables the calculation of the individual  $U/i$  curves and voltage losses (overpotential) in the fuel cell and the determination of the rate determining reaction steps depending on current density and humidification.

#### References

1. Daimler-Benz, HighTech Report'97, p. 20.
2. D. Bevers, N. Wagner and M. von Bradke, *Int. J. Hydrogen Energy* **23** (1997) 57.
3. D. Bevers and N. Wagner, *Patent DE 19509749 C2* (1997).
4. T.A. Zawodzinski Jr., A. Han, M. Minnema, J. Valerio and S. Gottesfeld, *Proc. Electrochem. Soc.* **23** (1994) 190.
5. N. Wagner, E. Gülzow, B. Müller and C.A. Schiller, Proc. 51st ISE Meeting, Warsaw, Poland (2000).
6. C.A. Schiller, F. Richter, E. Gülzow and N. Wagner, *Phys. Chem. Chem. Phys.* **3** (2001) 374.
7. N. Wagner, W. Schnurnberger, B. Müller and M. Lang, *Electrochim. Acta* **43** (1998) 3785.
8. N. Wagner, E. Gülzow, M. Schulze and W. Schnurnberger, in H. Steeb and H. Abaoud (Eds), 'Hysolar' (Stuttgart, 1996), p. 161.
9. C. Gabrielli, 'Use and Applications of Electrochemical Impedance Techniques', Technical Report 24, Solartron Instruments (1990).
10. M. Lang, R. Henne, G. Schiller and N. Wagner, in Proceedings of the 5th International Symposium on 'SOFC', Proc. Vol. 97-40, The Electrochemical Society (1997) p. 461.
11. C.A. Schiller, F. Richter, E. Gülzow and N. Wagner, *Phys. Chem. Chem. Phys.* **3** (2001) 2113.